Practical Laboratory Medicine 45 (2025) e00464

Contents lists available at ScienceDirect

Practical Laboratory Medicine

journal homepage: www.elsevier.com/locate/plabm

Research Article

Integrative analysis of exosomal ncRNAs and their regulatory networks in liver cancer progression

Farzin Mirzaei-nasab [a,b], Ahmad Majd [a], Yousef Seyedena [a], Nazanin Hosseinkhan [c,*], Najma Farahani [d,**], Mehrdad Hashemi [d,e,***]

[a] Department of Genetics, Faculty of Biological Sciences, North Tehran Branch, Islamic Azad University, Tehran, Iran, Sure
[b] Basic and Molecular Epidemiology of Gastrointestinal Disorders Research Center, Research Institute for Gastroenterology and Liver Diseases, Shahid Beheshti University of Medical Sciences, Tehran, Iran
[c] Endocrine Research Center, Institute of Endocrinology and Metabolism, Iran University of Medical Sciences, Tehran, Iran
[d] Farhikhtegan Medical Convergence Sciences Research Center, Farhikhtegan Hospital Tehran Medical Sciences, Islamic Azad University, Tehran, Iran
[e] Department of Genetics, Faculty of Advanced Science and Technology, Tehran Medical Sciences, Islamic Azad University, Tehran, Iran

ARTICLE INFO

Keywords:
Hepatocellular carcinoma
Systems biology
Exosomes
Non-coding RNA
Liver cancer
Biomarkers

ABSTRACT

Background: Hepatocellular carcinoma (HCC) is a significant global health challenge with complex molecular underpinnings. Recent advancements in understanding the role of non-coding RNAs (ncRNAs) and exosomes in cancer biology have opened new avenues for research into potential diagnostic and therapeutic strategies.

Methods: This study utilized a comprehensive approach to analyze gene expression patterns and regulatory networks in HCC. We integrated RNA sequencing data gathered from both tissue samples and exosomes. The WGCNA and limma R packages were employed to construct co-expression networks and identify differentially expressed ncRNAs, including long non-coding RNAs (lncRNAs) and circular RNAs (circRNAs).

Results: Our analysis demonstrated distinct expression profiles of various ncRNAs in HCC, revealing their intricate interactions with cancer-related genes. Key findings include the identification of a network of microRNAs that interact with selected lncRNAs and their potential roles as biomarkers. Moreover, exosomal RNA was shown to effectively reflect tissue-specific gene expression changes.

Conclusions: The results of this study highlight the significance of exosomal ncRNAs in the progression of liver cancer, suggesting their potential as both diagnostic biomarkers and therapeutic targets. Future research should focus on the functional implications of these ncRNAs to further elucidate their roles in HCC and explore their applications in clinical settings.

* Corresponding author.
** Corresponding author.
*** Corresponding author. Farhikhtegan Medical Convergence Sciences Research Center, Farhikhtegan Hospital Tehran Medical Sciences, Islamic Azad University, Tehran, Iran.
E-mail addresses: hosseinkhan@ut.c.ir (N. Hosseinkhan), Najmafarahani@gmail.com (N. Farahani), drmehashemi@iautmu.ac.ir (M. Hashemi).

https://doi.org/10.1016/j.plabm.2025.e00464
Received 5 December 2024; Received in revised form 19 January 2025; Accepted 7 March 2025
Available online 21 March 2025

1. Introduction

Liver cancer, particularly hepatocellular carcinoma (HCC), affects nearly one million people annually and is a leading cause of cancer-related deaths worldwide, especially among men aged 60 to 80, and in regions with high rates of liver diseases like cirrhosis, hepatitis B, and hepatitis C [1]. Early detection relies on understanding its genetic and molecular causes. Cancer arises from genetic abnormalities that drive rapid proliferation, metastasis, and drug resistance by altering molecular pathways within the tumor microenvironment, significantly facilitated by exosomes [2].

Exosomes, small vesicles that facilitate intercellular communication, carry diverse biomolecules such as proteins, lipids, and nucleic acids, influencing recipient cell behavior [3]. They contain non-coding RNAs (ncRNAs) like long non-coding RNAs (lncRNAs) and circular RNAs (circRNAs), which are crucial in regulating gene expression and forming complex regulatory networks through mechanisms like the ceRNA hypothesis [4].

Exosomal ncRNAs, including LncRNAs and miRNAs, play critical roles in cancer by modulating gene expression and influencing tumor progression and metastasis [5–8]. Understanding these roles is vital for developing new diagnostic tools and therapies for cancer treatment [9]. Exosomal circRNAs, for instance, are key regulators influencing cancer proliferation, invasion, and drug resistance [10].

Studies highlight the unique protein and RNA profiles of exosomes from HCC cells, underscoring their functional impact on the tumor microenvironment and cancer progression [2,4,11]. These exosomes reshape the tumor microenvironment, promoting tumor progression and immune evasion, critical considerations for cancer treatment and immunotherapy [12,13].

Exosomes serve as potential biomarkers for monitoring tumor advancement and treatment response due to their stability and specificity in reflecting cancer status and progression [2,4,14]. Despite extensive research on exosomal ncRNAs in cancer biology, there remains a notable gap regarding their specific roles in HCC [15], particularly in interactions and regulatory mechanisms.

This study seeks to explore the expression patterns and interactions of ncRNAs within exosomes from liver cancer patients to fill the existing research gap. Using computational analyses, exploring ncRNA expression profiles and their potential as biomarkers for early detection and therapeutic targeting in HCC, this study. By filling this gap, this research contributes to a deeper understanding of liver cancer pathogenesis and highlights potential diagnostic and therapeutic avenues.

In summary, this study focuses on constructing co-expression networks and investigating regulatory mechanisms of exosomal ncRNAs in HCC. Through comprehensive analyses, aiming to identify novel biomarkers and elucidate the roles of exosomal ncRNAs in liver cancer progression, thereby contributing to a deeper understanding of liver cancer pathogenesis.

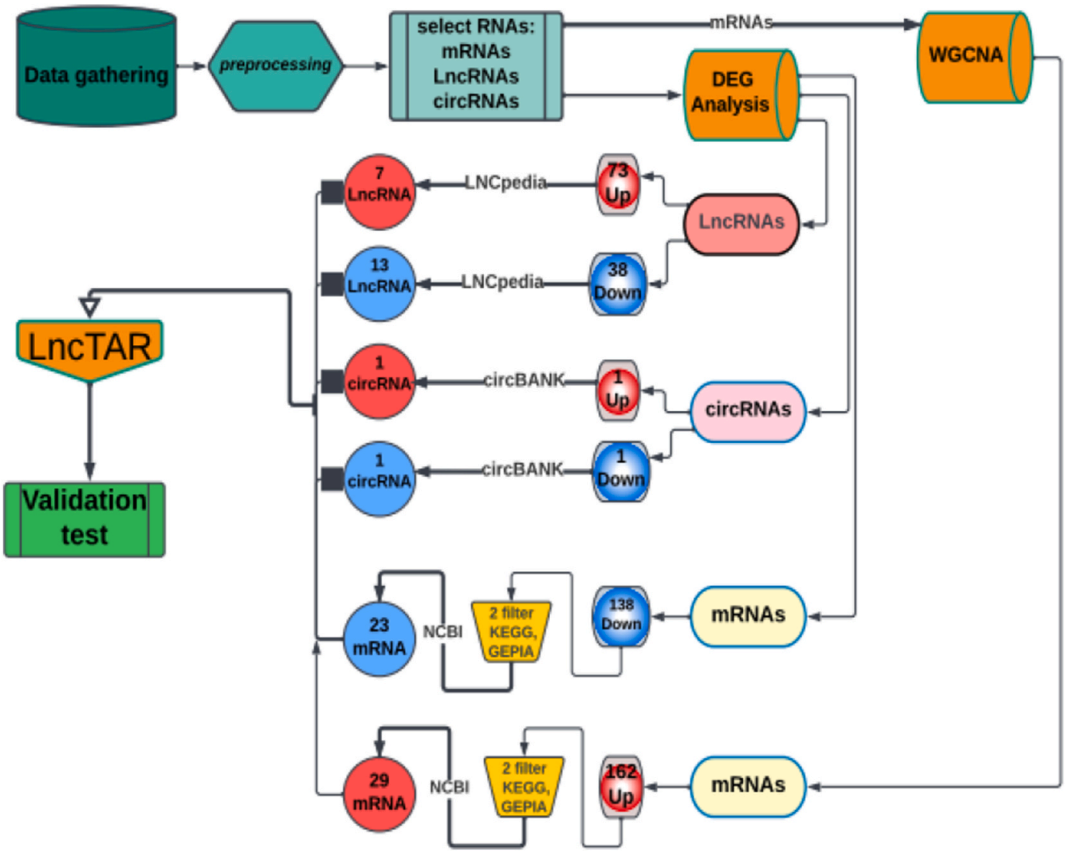

Fig. 1. Flowchart illustrating steps in systems biology analyses.

2. Materials and methods

2.1. Gene expression profile

Gene expression data is pivotal for reconstructing gene regulatory networks and elucidating gene regulatory interactions. The RNA sequencing (RNA-seq) data used in this study were sourced from the hepatocellular carcinoma (HCC) dataset available in the exoRbase database (version 1), accessible at http://www.exorbase.org. The gene expression data were pre-processed to obtain normalized transcripts per million (TPM) values directly from the RNA-seq dataset. Specifically, the normalization process ensured that gene expression levels were comparable across samples, thereby facilitating a comprehensive analysis integrating cancerous and healthy sample datasets.

2.2. Analysis of genes with the most significant expression changes (gene filtering)

To construct co-expression networks using the WGCNA package in R, a subset of genes was filtered out due to limited mRNA availability. Initially, genes with an average expression lower than 2 TPM were excluded from the dataset. Then, a log transformation ($\log(x+1)$) was applied to the gene expression data to normalize it. To enhance data quality and minimize errors, a variance-based filtering approach was utilized [16,17]. Subsequently, the variance of genes was calculated, and the genes were sorted in descending order based on their variance. The top 5000 genes exhibiting the highest variance were selected for constructing the co-expression network [18].

The schematic representation of the overall flowchart for conducting systems biology analyses is presented in Fig. 1. This flowchart outlines the main steps in conducting systems biology analyses.

2.3. Reconstruction of WGCNA network

For the construction and analysis of a co-expression network from the selected mRNA genes in this study, the WGCNA package (version 1.72–1) in the R language (version 4.3.0, developed by the GNU Project) was used. The superiority of the WGCNA method over other approaches, such as partial correlation and the Partial Correlation with Information Theory (PCIT), has been demonstrated. In the WGCNA method, genes with high correlation, whose expression values are close to each other, are functionally involved in similar biological processes and pathways. Therefore, they can be grouped into common network modules.

Using the pre-processed selected mRNAs from the previous stage, which includes 5000 genes for HCC and healthy samples, a co-expression network in the form of a signed hybrid was reconstructed using the WGCNA package. To construct the network, a similarity matrix was generated by calculating the Pearson correlation between all pairs of genes. To achieve a scale-free topology, the similarity matrix was raised to the power of β, which was set to 5. The adjacency matrix was then obtained. The selection of β was based on the suggested scale-free topology criteria by Ref. [19], resulting in an appropriate scale-free topology index (R^2) of 0.92, indicating the biological relevance of the network.

Using the adjacency matrix, a Topological Overlap Matrix (TOM) was calculated. This similarity measure indicates the correlation and overlap between neighboring nodes, which is useful in biological networks [20]. To identify biologically meaningful modules, the TOM was transformed into a Topological Overlap Dissimilarity Matrix (TOM dissimilarity) by subtracting it from 1. A hierarchical clustering tree (dendrogram) of genes was generated based on the TOM dissimilarity [20]. Finally, modules representing highly interconnected clusters of co-expressed genes were obtained by cutting the dendrogram branches using the Dynamic Tree Cut algorithm [21]. In the next step, the most significant module was selected for further analysis.

To select the best module, an eigengene, which is the first principal component of its expression matrix, was calculated for each module. This eigengene serves as a summary indicator for each module, reflecting expression changes in a one-dimensional vector. These eigengenes were then used to calculate the module-trait relationships. The primary clinical feature examined was the sample type, i.e., cancer versus normal samples. The module-trait relationship for a specific module and trait is the correlation between the eigengene of the module and the trait vector for all samples. Subsequently, a module (yellow) with the highest correlation with the sample type trait and the lowest *p*-value was selected. Finally, genes involved in cell cycle pathways or apoptosis were chosen.

2.4. MM-GS analysis

In the MM-GS analysis, the WGCNA package in R was utilized. From the modules identified through WGCNA analysis, the yellow module was selected as it showed the strongest correlation with disease traits, as illustrated in Fig. 2-I. The yellow module contained genes that were highly interconnected and demonstrated significant correlation with the disease phenotype. The GS-MM analysis was then conducted using all genes within this yellow module to identify key genes associated with disease progression.

2.5. DEG analysis and interaction investigation with LncTAR

The differential expression analysis (DEG) of genes within modules was conducted using the limma package (Linear Models for Microarray Data) [22] in R. This analysis included mRNA, LncRNA, and circRNA data, with the exclusion of records containing zero values. mRNA sequences were obtained from

https://www.ncbi.nlm.nih.gov/, LncRNA sequences from https://lncipedia.org/, and CircRNA sequences from http://www.

circbank.cn/, all in FASTA format.

To examine the interactions between mRNA, LncRNA, and circRNA, the LncTAR tool was employed [23] LncTar serves as a valuable tool for researchers investigating interactions between RNAs.

2.6. Gene ontology analysis and pathway enrichment

In this study, the KEGG [24] and EnrichR databases [25] were used for the interpretation and analysis of genes associated with significant candidate modules.

2.7. Comprehensive analysis of LIHC OMICS data

The UALCAN web resource (https://ualcan.path.uab.edu) [26] was used to conduct an extensive analysis of LIHC OMICS data. The focus was on genes identified through WGCNA and differential expression analysis, targeting the upregulated and downregulated gene expression patterns in exosomes. This platform provided a vast array of information, including sample sizes, cancer stages, gender distribution, and histological subtypes within LIHC datasets. This comprehensive analysis allowed to understand the expression patterns of identified genes and compare the results effectively.

2.8. Online databases and tools used for mRNAs and ncRNAs analysis

Several online databases and tools were employed to analyze the data, including databases for examining lncRNAs, circRNAs, microRNAs, protein-protein interactions, pathway enrichment, and data visualization. A detailed description of all databases and tools used in this study, along with their specific applications and web addresses, is provided in Appendix 8.

We identified potential interactions between our selected genes and microRNAs using the miRTarBase database. We found that 24 microRNAs interacted with 7 of our selected genes. We then extended this analysis to include physical interactions between these microRNAs and our remaining genes, as well as with 10 lncRNAs and 1 circRNA. The interactions were visualized using Cytoscape software in Fig. 4.

3. Results

3.1. Data collection, normalization, and outlier removal

RNA-Seq data for normal and liver cancer exosomes were extracted from the exoRbase database (GSE100206, GSE100207). This dataset includes 32 samples from individuals with liver cancer and 21 samples from healthy individuals. After downloading, data quality was assessed using the Plot density function to visualize expression levels, as shown in Fig. 2-A.

Hierarchical clustering, performed using the hclust command, further assessed data quality. The results are presented in Fig. 2-B. This method identifies and removes outliers; however, no outliers were found, indicating the data's robustness. The specific codes used are provided in Appendix 1.

3.2. Identification of WGCNA modules

The optimal beta value for constructing a Scale-Free network based on gene expression profiles was calculated. These values and the mRNA data results are depicted in Fig. 2-C and 2-D. Subsequently, co-expression networks for cancerous and healthy data were reconstructed and clustered, assigning a unique color to each module. The gray module, representing unclustered genes, was discarded. The modules for hepatocellular carcinoma (HCC) are shown in Fig. 2-E.

An eigengene, representing each module's gene expression profile, was assigned. Hierarchical clustering of module representatives for HCC disease was performed to identify closely correlated modules, as seen in Fig. 2-F. No modules were combined.

To determine the most significant modules, a module-trait correlation analysis was performed on the obtained modules for HCC disease. The results of this analysis can be observed in Fig. 2-G.

Module-trait correlation analysis identified significant modules for HCC disease, presented in Fig. 2-G. The co-expression patterns of genes within the Yellow module are shown in Fig. 2-H, suggesting potential functional relationships or regulatory interactions within this module.

The results of the module membership (MM) and gene significance (GS) analysis for the Yellow module are detailed in Fig. 2-I, showing a significant correlation coefficient of 0.96 with a *p*-value of 6e-29. Additional module information is provided in Appendix 2.

3.3. Gene ontology analysis of the candidate module in HCC disease using EnrichR

Significant pathways from biological and gene ontology pathways related to the Yellow module were obtained using EnrichR. These results are reported in Fig. 2-J, with a complete gene ontology analysis provided in Appendix 3. Fig. 2-K presents the KEGG 2021 Human database enrichment results for the Yellow module, indicating significant pathways.

Genes involved in significant pathways were selected through enrichment analysis. Two additional filters were applied: KEGG pathways related to cell cycle or apoptosis, and upregulation in cancer tissue samples as determined by GEPIA. A list of 29 genes,

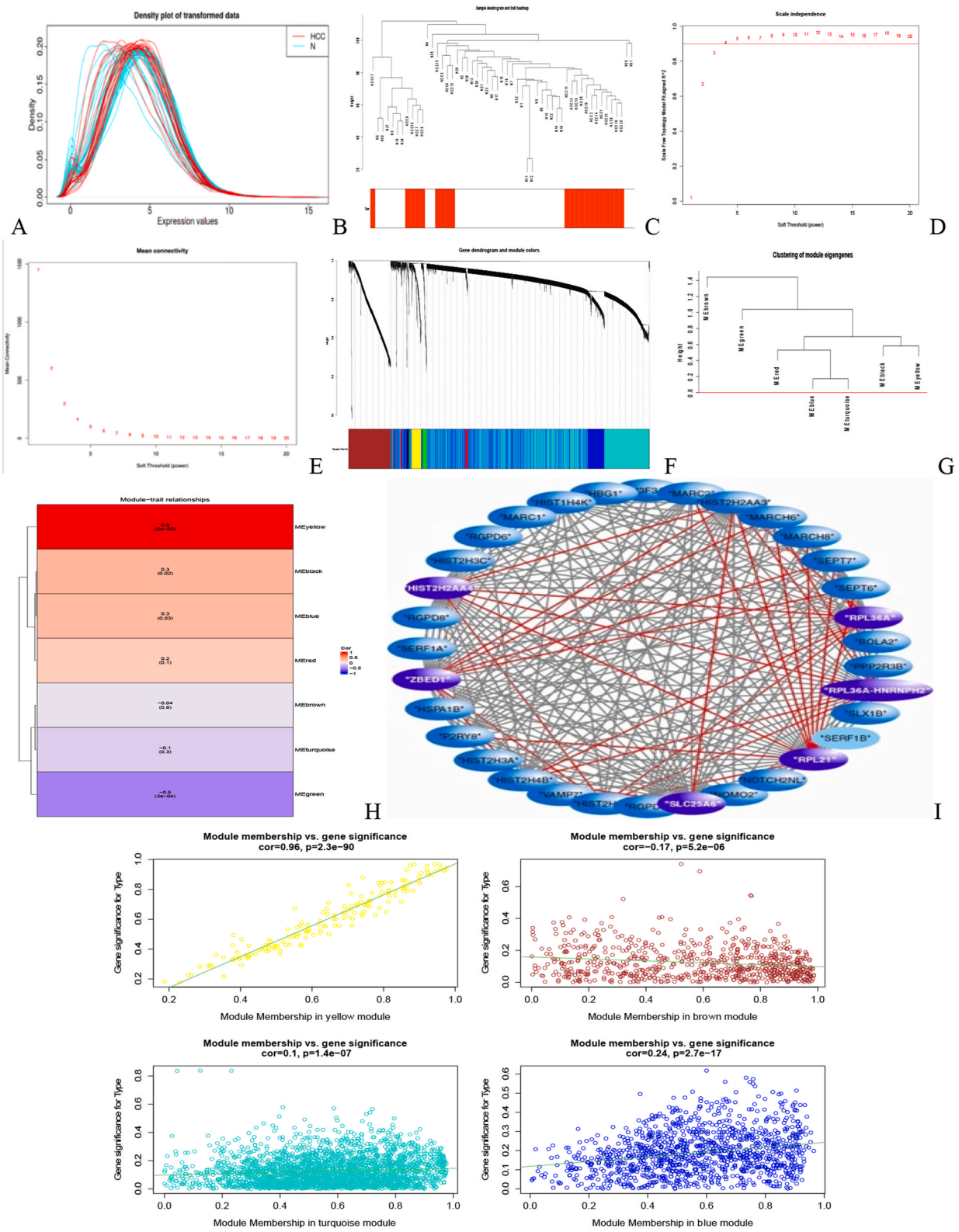

Fig. 2. Workflow integrating WGCNA, DEG analysis, and enrichment studies in hepatocellular carcinoma (HCC). (A) RNA expression intensity in HCC. (B) Hclust analysis of mRNA data between HCC and normal stages. (C–D) Optimal beta selection and network topology in Scale-Free biological networks for normal-HCC mRNA data. (E) Modules identified in HCC mRNA data. (F) Dendrogram clustering of module representatives. (G)

Module-trait correlation analysis. (H) Co-expression in the Yellow module by WGCNA. (I) Module membership and gene importance analysis in Normal-HCC mRNA data. (J) Biologically significant pathways and gene ontology related to the Yellow module by EnrichR [29]. (K) KEGG enrichment of genes in the Yellow module [25,30,31]. (L) Comparison of LogFc + genes with WGCNA's Yellow module output by Venny tool [32]. (M) Enrichment analysis of DEG− genes by Enrichr [29]. (N) KEGG enrichment of DEG− genes [25,30,31]. (O) Graphical network of top 10 diseases related to Hepatocellular Carcinoma [28].

corresponding to 70 different transcripts based on NCBI/Ref-seq annotations, was obtained (Table 1).

The KEGG pathway enrichment analyses for this study were performed using EnrichR (https://maayanlab.cloud/Enrichr/). Figures related to KEGG pathways (Fig. 2J and K-M-N) were generated using data accessed through EnrichR, which provides KEGG pathway information for research purposes.

3.4. Differential expressed genes (DEGs) in mRNAs

Comparing logFC + genes with the Yellow module genes from the WGCNA network revealed complete overlap, indicating these genes are upregulated co-expression genes (Fig. 2-L). DEG analysis, excluding genes with zero mean expression, identified downregulated genes using the Limma package in R. Genes with an adjusted p-value <0.01 were considered downregulated. Further insights are provided in Appendix 4.

Out of 263 significant genes based on adjusted p-value, 138 were downregulated. Significant pathways associated with these DEGs were obtained using EnrichR, shown in Fig. 2-M and 2-N. Genes involved in the cell cycle and apoptosis pathways, and exhibiting downregulation according to GEPIA, were selected (Table 2). Differential expression analysis results for mRNAs, LncRNAs, and circRNAs are in Appendix 5.

Next, the DEGs Down was examined to identify those involved in cell cycle regulation or apoptosis based on KEGG [27] information. Then, using the data available in the GEPIA database, those genes showing downregulation were selected (Table 2). Label 1 indicates that the gene of interest is involved in important cell cycle pathways. Label −1 represents genes with downregulation according to the GEPIA database. Label 0 indicates cases where none of the mentioned results were observed.

Fig. 2-O illustrates a graphical network representing the top 10 diseases associated with hepatocellular carcinoma. In this network, nodes represent the diseases, and the connections or edges between nodes indicate the relationships or associations between these diseases. The nodes or edges' size, color, or other visual attributes provide additional information about the strength or nature of these relationships. By examining this graphical network, insights can be gained into the interconnectedness and potential comorbidities of the top diseases linked to hepatocellular carcinoma.

Figures J-K-M-N. KEGG pathway analysis for HCC samples. The KEGG pathway enrichment analyses presented in these figures were performed using EnrichR (https://maayanlab.cloud/Enrichr/). EnrichR provides access to KEGG pathway data for research purposes, and the visualizations were generated directly from this resource.

3.5. Differential expressed genes (DEGs) in HCC-LncRNAs

Genes were filtered to remove those with zero expression average. The Limma package in R identified significant DEGs with an adjusted p-value <0.01. Among 111 significant DEGs, 73 were upregulated and 38 downregulated. DEGs with available sequences in the Lncpedia database are shown in Fig. 3-A and 3-B.

3.6. Differential expressed genes in HCC-CircRNA data

From the significant DEGs, one gene showed increased expression and one decreased expression. The FASTA sequences of these genes can be obtained from the CircBANK database, as shown in Fig. 3-C.

The analysis was performed using the R programming language with the following packages: igraph, rTRM, and png. In Fig. 4, a two-part network illustrating the influence of differentially expressed genes (DEG+ and DEG−) CircRNAs and LncRNAs on the Yellow module and DEG− mRNAs is presented. The interactions between these RNAs are depicted.

As shown in Fig. 4, this image was generated using Cytoscape [33]. The figure illustrates mRNAs that overlap with non-coding RNAs (ncRNAs). UP mRNAs are identified based on their interactions with DEG− and DEG + ncRNAs, and Down mRNAs are also selected based on their interactions with both types of ncRNAs. The color-coding represents expression patterns from exosomal RNA-seq data, showing how these genes are expressed differently in HCC exosomes compared to normal controls.

Tables of the interaction results between mRNAs with upregulated and downregulated LncRNAs and circRNAs are provided in Appendix 6.

3.7. Results of physical interaction analysis

The results of the physical interaction analysis are presented in Table 3. For the upregulated and downregulated messenger RNAs (mRNAs), multiple transcript variants were identified for each gene. Due to the high sequence overlap among different transcript variants, only the gene names are listed here. Following the physical interaction analysis, a total of 166 common interactions were selected out of eight corresponding interactions.

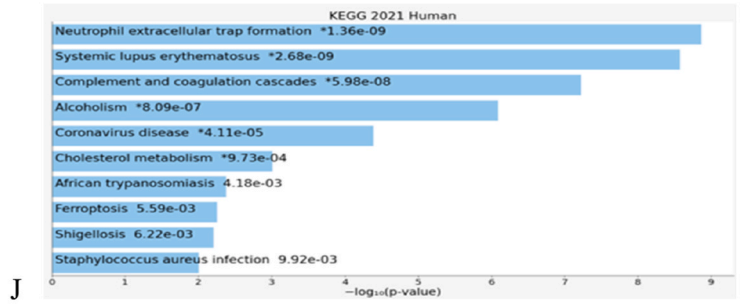

J

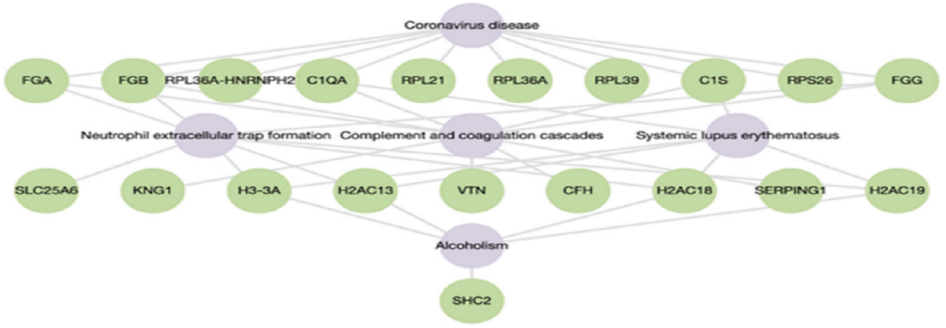

K

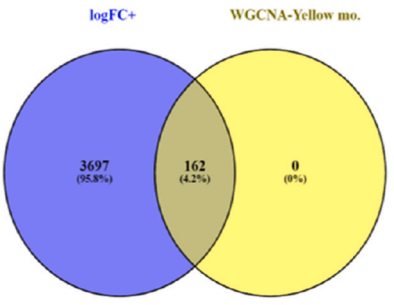

L

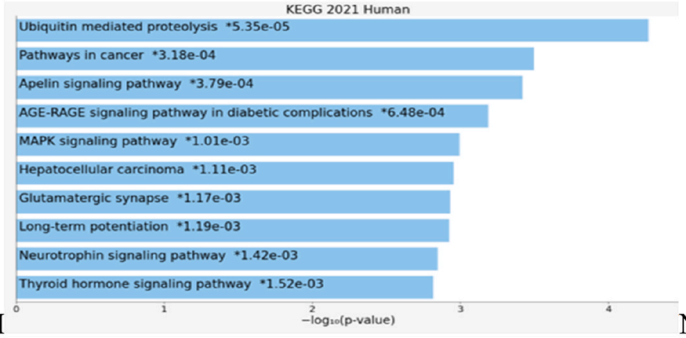

M N

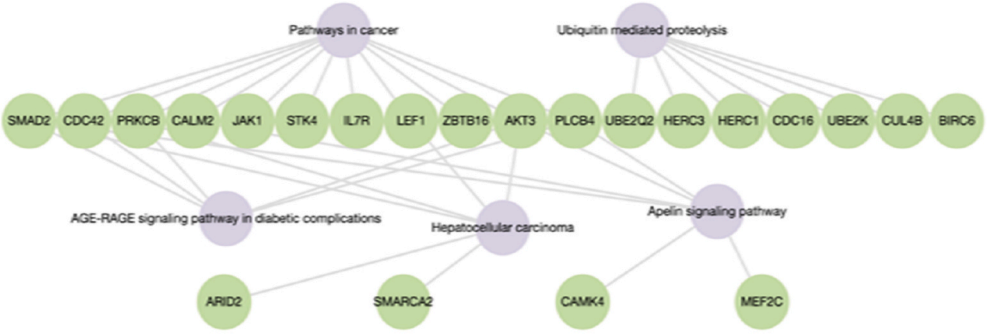

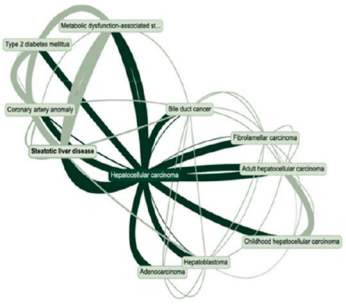

O

Fig. 2. (*continued*).

Table 1
Genes in the yellow module output from WGCNA analysis identified as up-regulated using KEGG [28] and GEPIA filters.

Gene Symbol	Module Color	GS.Type	p.GS.Type	MM.yellow	p.MM.yellow
ZBED1	yellow	0.962079	1.94E-30	0.957347208	3.68E-29
SLC25A6	yellow	0.934238	1.73E-24	0.959161976	1.24E-29
HSPA1B	yellow	0.911247	2.73E-21	0.924771055	4.77E-23
FGB	yellow	0.844718	1.87E-15	0.875982192	8.96E-18
ORM1	yellow	0.811584	1.69E-13	0.853134586	5.01E-16
HRG	yellow	0.774312	1.04E-11	0.812141095	1.58E-13
PPP2R3B	yellow	0.757742	5.08E-11	0.78879904	2.31E-12
FGG	yellow	0.700765	5.15E-09	0.725556917	7.95E-10
APOB	yellow	0.698028	6.26E-09	0.750443977	9.83E-11
MYL6B	yellow	0.685911	1.45E-08	0.690707819	1.04E-08
CYP2E1	yellow	0.684578	1.58E-08	0.761483469	3.59E-11
FGA	yellow	0.665319	5.49E-08	0.698225432	6.17E-09
APOA2	yellow	0.642471	2.15E-07	0.686138183	1.42E-08
RASA4B	yellow	0.625151	5.61E-07	0.7402919	2.37E-10
GC	yellow	0.603415	1.73E-06	0.660054814	7.59E-08
ALDOB	yellow	0.564663	1.06E-05	0.617653376	8.36E-07
RASA4	yellow	0.557154	1.47E-05	0.675856122	2.81E-08
ALB	yellow	0.556889	1.49E-05	0.711233717	2.40E-09
KNG1	yellow	0.552543	1.79E-05	0.636929549	2.94E-07
APOH	yellow	0.522358	6.02E-05	0.581176983	5.04E-06
COL4A1	yellow	0.515986	7.67E-05	0.584020417	4.42E-06
SHC2	yellow	0.501379	0.000131	0.563830264	1.10E-05
TF	yellow	0.489262	0.000201	0.549825919	2.00E-05
KCNJ2	yellow	0.429778	0.00132	0.537655923	3.30E-05
SCD	yellow	0.422299	0.001634	0.570159477	8.32E-06
VTN	yellow	0.416662	0.001913	0.493096134	0.000175915
INSR	yellow	0.401905	0.002854	0.496066222	0.000158468
CXCR5	yellow	0.334518	0.014355	0.396558594	0.00328509
MGST1	yellow	0.291656	0.034093	0.401906994	0.002853903

Table 2
The list of significant down-regulated DEGs based on the KEGG and GEPIA filters.

	KEGG	GEPIA	logFC	adj.P.Val
FYB	1	−1	−201.4101662	6.35E-05
PRKCB	1	−1	−98.67789065	0.000244
KAT6A	1	−1	−89.64292823	1.86E-06
PLEK	1	−1	−83.19481878	0.00947
NCOR1	1	−1	−72.44780179	2.47E-06
IL7R	1	−1	−70.23576777	0.00707
SMARCA2	1	−1	−69.18246396	0.001513
AKT3	1	−1	−63.84605529	3.20E-06
LEF1	1	−1	−55.75956944	0.002092
BIRC6	1	−1	−43.6924995	0.003107
THOC2	1	−1	−41.68583865	1.14E-05
RSF1	1	−1	−41.45360285	0.007161
BTK	1	−1	−37.07722659	0.001807
DNMT1	1	−1	−35.55202429	0.002048
CRKL-1	1	−1	−27.23454566	0.005057
HDAC9	1	−1	−25.50142416	3.28E-05
TTN	1	−1	−21.24324449	0.001597
USP10	1	−1	−20.39936841	0.006471
CAMK4	1	−1	−19.40384265	0.001341
ARID2	1	−1	−18.395143	0.008518
RAB14	1	−1	−16.85863442	0.001031
DLG1	1	−1	−14.98564783	0.00984
PPP2R2D	1	−1	−12.1515161	0.007608
ZBTB16	1	−1	−10.78785871	0.000626
HPGD	1	−1	−9.875168146	0.004836
PLCB4	1	−1	−8.936647911	0.00169
MEF2C	1	−1	−60.46365042	3.89E-07

Based on the selection of genes with interactions and overlap with both positive and negative differentially expressed gene (DEG) non-coding RNAs (ncRNAs), the upregulated genes were searched first, followed by the downregulated genes, in various sources (Tables 3 and 4). Furthermore, the important pathways involved in the cell cycle, which undergo changes leading to cancer, were also examined.

A

LncRNA+	Numbers of transcripts recorded in LNCipedia	logFC	AveExpr	t	P.Value	adj.P.Val
RN7SL1	2	27186	43330	9,6771	3,21E-13	2,71E-11
RP11-144G6.12	2	7,7702	5,5449	8,618	1,37E-11	7,02E-10
BMS1P2	1	8,163	5,1676	9,4534	7,02E-13	5,41E-11
CH507-513H4.6	1	4,8705	2,828	6,6639	1,70E-08	5,30E-07
CH507-513H4.4	1	56,882	28,8	6,3889	4,67E-08	1,38E-06
CH507-528H12.1	1	3,8837	2,0684	5,5198	1,09E-06	3,07E-05
RP11-514P8.8	1	3,5486	4,2241	4,9686	7,69E-06	0,000193
CTD-2031P19.4	0	61,837	30,773	15,086	1,25E-20	1,48E-17
GTF2IP4	0	43,762	41,813	12,577	2,16E-17	8,50E-15
NUDT4P2	0	20,318	8,0581	12,627	1,85E-17	8,50E-15

B

LncRNA -	Numbers of transcripts recorded in LNCipedia	logFC	AveExpr	t	P.Value	adj.P.Val
VIM-AS1	18	-70,2	72,479	-5,263	2,73E-06	7,15E-05
EAF1-AS1	15	-7,491	4,7205	-3,697	0,000527	0,006955
RP11-513I15.6	8	-27,18	20,714	-3,701	0,000521	0,006955
AC009120.6	6	-20,72	12,948	-3,74	0,000461	0,006398
SEMA3F-AS1	4	-5,343	3,4172	-3,695	0,00053	0,006955
RP11-796E2.4	3	-23,76	22,101	-3,562	0,000799	0,008816
RP11-367I11.2	1	-12,57	8,0939	-3,881	0,000294	0,004699
RP11-3P17.4	1	-54,79	33,253	-3,727	0,000479	0,006584
RP11-474G23.2	1	-8,8	5,5033	-3,687	0,000542	0,00704
RP11-96D1.11	1	-3,993	2,8773	-3,675	0,000564	0,007165
AC021224.1	1	-49,53	31,427	-3,642	0,000624	0,007676
RP3-394A18.1	1	-6,567	5,0855	-3,639	0,00063	0,007676
MYCBP2-AS1	1	-3,204	2,0603	-3,633	0,000643	0,007744
XXbac-BPG252P9.9	1	-13,31	9,4175	-3,57	0,00078	0,008771
TUG1	0	-13,73	53,629	-3,75	0,000447	0,006355
RP11-983P16.4	0	-13,28	14,641	-3,655	0,000599	0,007451
CTD-2231E14.8	0	-22,04	14,545	-3,84	0,000336	0,005019
CTC-250I14.6	0	-3,751	2,6994	-3,606	0,000697	0,008151

C

ExoRbase ID	CircBase ID	logFC	AveExpr	t	P.Value	adj.P.Val	significant	Hosted Gene symbol
exo_circ_000760	hsa_circ_0001380	-1624,1193	1019,1803	-7,5191736	6,96E-10	1,59E-05	sig	UBXN7
exo_circ_001027	hsa_circ_0073052	248,999024	129,105491	5,69267076	5,70E-07	0,00651046	sig	POLK
exo_circ_000016		4568,21947	13531,1318	4,27535547	8,08E-05	0,61492539	notsig	
exo_circ_000006		-2373,3876	14927,5577	-4,0766587	0,00015544	0,65130615	notsig	
exo_circ_000012		-1172,0108	5241,49213	-1,4833094	0,14396981	0,65130615	notsig	

Fig. 3. Differential expression of genes (DEGs) in HCC involving LncRNAs and circRNAs. (A) LncRNA DEG + genes with corresponding FASTA sequences in the LNCipedia database. (B) LncRNA DEG− genes with corresponding FASTA sequences in the LNCipedia database. (C) circRNA transcripts of DEG+ and DEG− available in circBase. Selected significant circRNAs for further analysis.

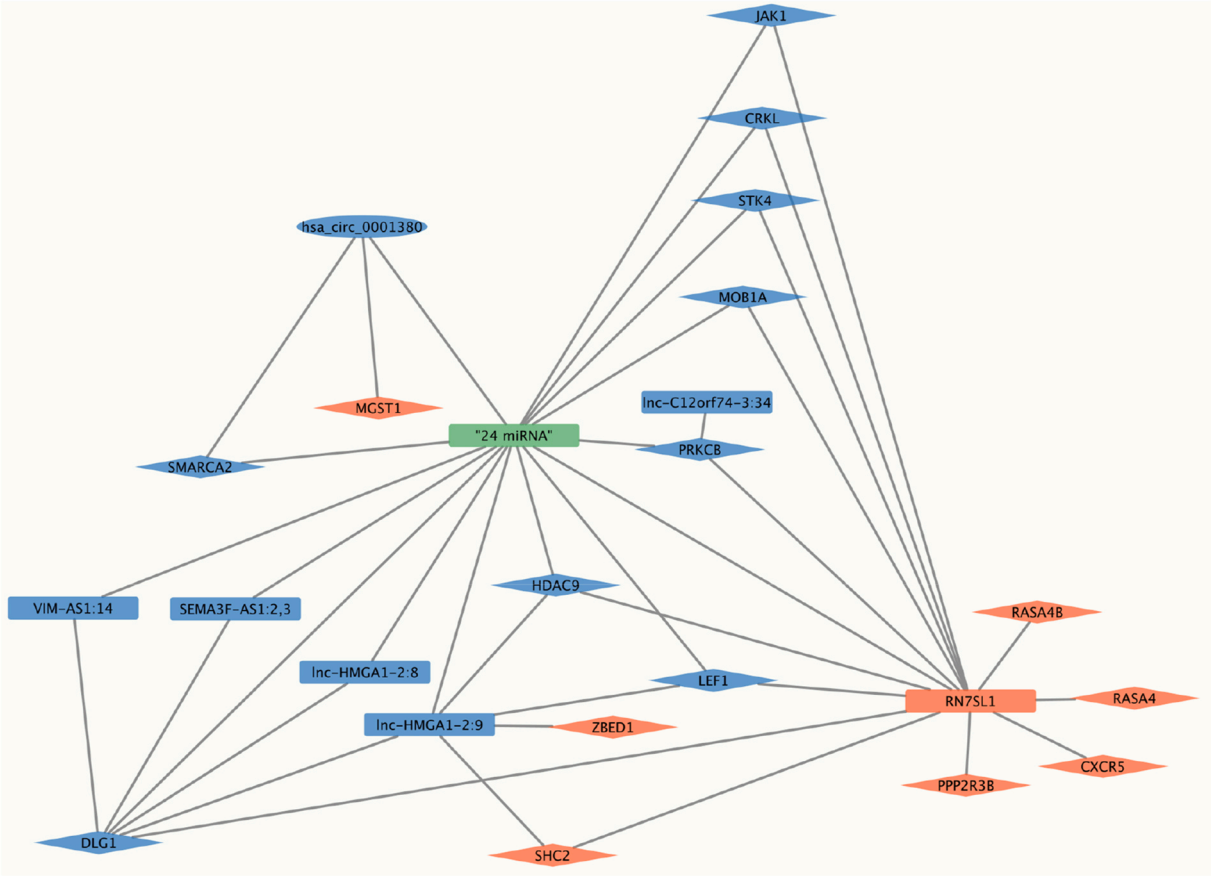

Fig. 4. Network visualization of RNA interactions in HCC. The "24 miRNAs" node represents a set of 24 distinct microRNAs. Upregulated genes are shown in red, while downregulated genes are depicted in blue. All genes and lncRNAs interact with all 24 miRNAs, while the circRNA interacts with 23 out of 24 miRNAs, lacking interaction only with *hsa-miR-30c-5p*.

Table 3
Upregulated genes examined across various cancers and cell cycle pathways.

Genes (Up Regulated)	Disorders	Pathway in KEGG
MGST1	**Liver cancer** [34], Stomach cancer [35],Pancreatic cancer [36], Colorectal cancer [37]	**Pathways in cancer, Hepatocellular carcinoma**
RASA4 RASA4B	**Liver cancer** [38], Cervical cancer [39], Brest cancer [40]	Ras signaling pathway
SHC2	**Liver cancer** [41],Brest cancer [42],Lung cancer [43]	**Alcoholism** Chemokine signaling pathway Chemokine signaling pathway
ZBED1	**Liver cancer** [46],Stomach cancer [44]	regulates cell proliferation [44,45]
CXCR5	**Liver cancer** [47],Lung cancer [48], Prostate cancer [49] Colorectal cancer [50],Stomach cancer [51]	Chemokine signaling pathway
PPP2R3B	**Liver cancer** [52],Melanoma [53],Breast cancer [54]	PI3K-Akt signaling pathway AMPK signaling pathway

Table 4
Downregulated genes examined across various cancers and cell cycle pathways.

Genes (Down Reg.)	Disorders	Pathway in KEGG
CRKL	**Liver cancer** [55], Lung cancer [56],Breast cancer [57], Stomach cancer [58], Cervical cancer [59]	Pathways in cancer ErbB signaling pathway MAPK signaling pathway Rap1 signaling pathway
DLG1	Liver cancer [60], colorectal cancer [61], ovarian cancer [62], prostate cancer [63]	Hippo signaling pathway T cell receptor signaling pathway
HDAC9	Liver Cancer [64], Breast Cancer [65], Lung Cancer [66]	**Alcoholism**
JAK1	Liver Cancer [67], Melanoma [68], Ovarian Cancer [62]	PI3K-Akt signaling pathway EGFR tyrosine kinase inhibitor resistance Hepatitis C NOD-like receptor signaling pathway
LEF1	Liver Cancer [69], Prostate Cancer [70], Colorectal Cancer [71]	Hippo signaling pathway, **Hepatocellular carcinoma** Pathways in cancer Wnt signaling pathway **Alcoholic liver disease**
MOB1A	Liver Cancer [72], Colorectal Cancer [73], Bladder Cancer [74]	Hippo signaling pathway
PRKCB	Liver Cancer [75], Ovarian Cancer [62]	Pathways in cancer EGFR tyrosine kinase inhibitor resistance MAPK signaling pathway mTOR signaling pathway
STK4	Liver Cancer [76],Thyroid Cancer [77], Prostate Cancer [78]	Pathways in cancer FoxO signaling pathway Ras signaling pathway MAPK signaling pathway
KAT6A	Liver Cancer [79], Ovarian Cancer [80]	Signaling pathways regulating pluripotency of stem cells
PLCB4	Liver Cancer [81], Neuroblastoma [82], Prostate Cancer [63]	cGMP-PKG signaling pathway Wnt signaling pathway Rap1 signaling pathway
SMARCA2	Liver Cancer [41], Lung Cancer [83], Pancreatic Cancer [84]	**Hepatocellular carcinoma** Thermogenesis

To analyze protein-protein interactions (PPIs), the Integrated Interactions Database (IID) web tool was utilized. Protein-protein interactions refer to the physical associations between proteins in a biological system, playing a crucial role in various cellular processes and biological pathway functions. In this context, the PPIs displayed in Fig. 5-A are specifically derived from analyzing selected messenger RNA (mRNA) molecules. Fig. 5-A visualizes the connections between proteins, represented as nodes, highlighting their interactions as edges or links between these nodes. By studying this network of PPIs, insights can be gained into the complex web of interactions among proteins, identifying key players or hubs critical for the underlying biological processes being studied.

Additionally, *hsa-miR-449a* and *hsa-mir-107*, identified through computational analysis and documented in the Human MicroRNA Disease Database (HMDD) as influencing the upregulation and downregulation of several genes were utilized. A PPI analysis was then conducted by integrating these target genes with selected gene expression data. This allowed for the identification of potential interactions and connections between the genes regulated by these microRNAs and the genes identified in this study, as shown in Fig. 5-B, providing deeper insights into their roles and relationships in hepatocellular carcinoma.

Fig. 6 presents the analysis of PPI annotations based on diseases (A) and tissues (B). In part A of Fig. 6, the focus is on understanding the associations between PPIs and diseases. The PPI annotations are mapped and linked to specific disease categories, allowing

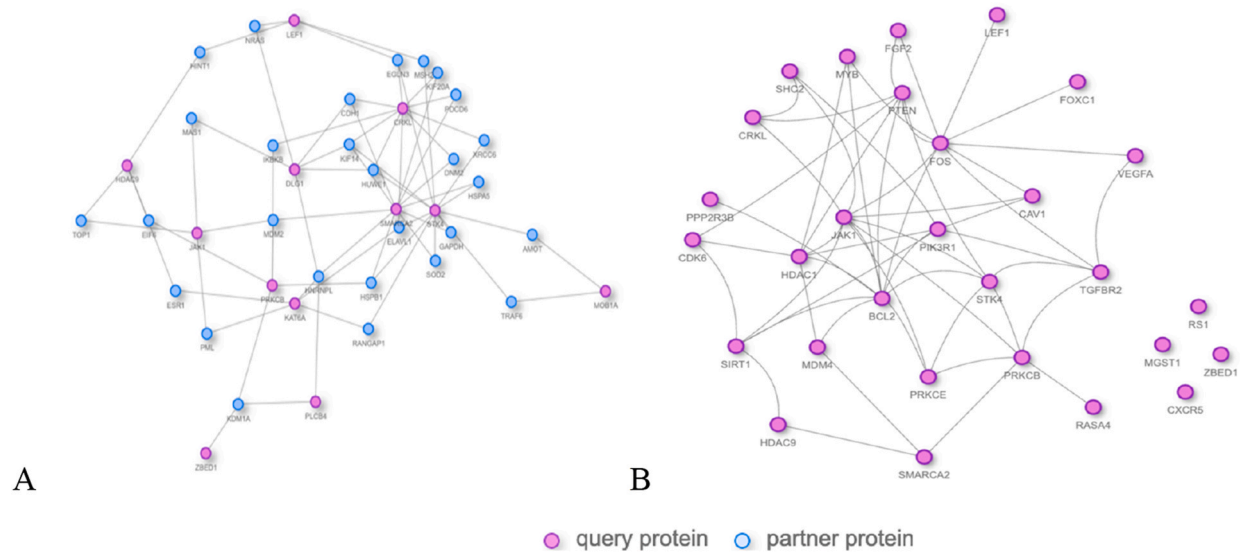

Fig. 5. (A) Protein-protein interactions (PPIs) based on selected mRNA profiles. (B) PPI network involving affected genes of *hsa-miR-449a* and *hsa-miR-107* with mRNA profiles in HCC.

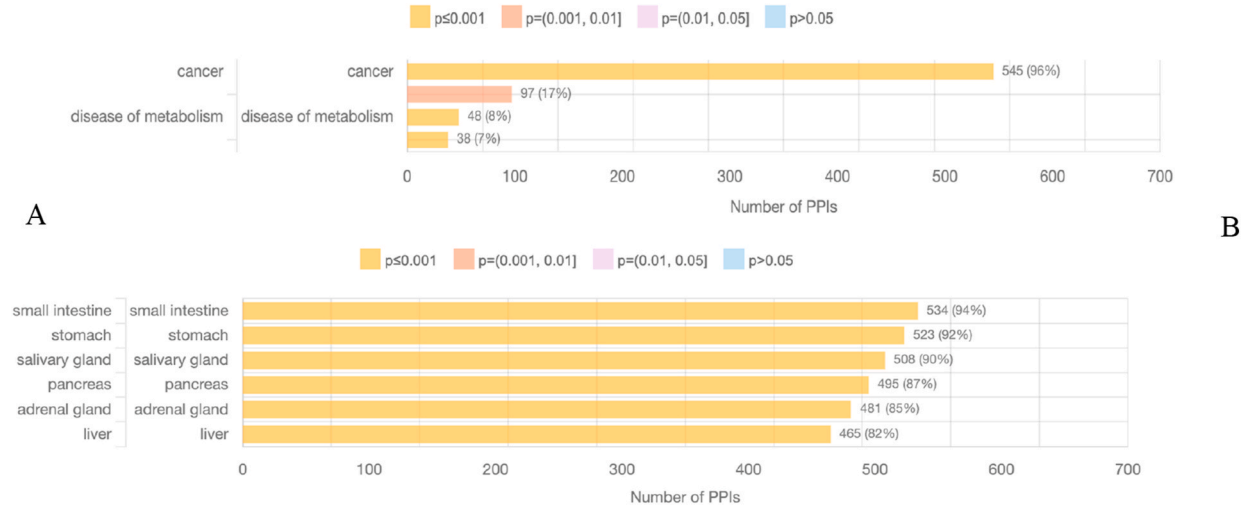

Fig. 6. (A) Analysis of PPI annotations based on diseases and (B) tissues.

exploration of the molecular basis and potential molecular targets associated with various diseases. By examining the PPIs within the context of diseases, insights can be gained into the underlying biological mechanisms, identifying disease-related protein modules or complexes, and potentially discovering novel therapeutic targets.

In part B of Fig. 6, the emphasis shifts to exploring the relationship between PPIs and specific tissues. By analyzing the PPI annotations within different tissue contexts, tissue-specific protein networks and interactions that play crucial roles in the physiological processes and functions of those tissues can be uncovered. This analysis provides valuable information about the molecular mechanisms underlying tissue-specific functions, potential biomarkers, and tissue-specific drug targets. The analysis of PPI annotations based on diseases and tissues in Fig. 6 offers a comprehensive view of the connections between protein interactions and specific disease categories or tissues. It helps understand the intricate relationships between proteins, diseases, and tissues, ultimately contributing to a deeper understanding of complex biological systems and facilitating the development of targeted therapeutic strategies.

The selected mRNAs at this stage were searched on the miRTarBase website [85]. Among the results, genes that had strong evidence according to quantitative polymerase chain reaction (qPCR), Western blot, and reporter assay criteria were chosen. These genes are indicated in Table 5. In addition to the names of the searched miRNAs, the expression patterns of miRNA and mRNA in UALCAN for LIHC were also searched, and the results are provided in the specified columns. It is worth noting that the genes listed in the mRNA column are those with decreased expression patterns in exosomes. The cases for which there were no results or were not statistically

Table 5
Investigation of physical interaction between RNA molecules and miRNA.

miRNA (miRTarBase)	LIHC Expression miRNA (UALCAN)	Target (mRNA)	LIHC Expression mRNA (UALCAN)
hsa-miR-29a-3p	Down	*CRKL*	Up
hsa-miR-124-3p	N/A	*CRKL*	N/A
hsa-miR-126-3p	Down	*CRKL*	N/A
hsa-miR-107*	Up	*CRKL*	N/A
hsa-miR-15a-5p	Up	*CRKL*	Up
hsa-miR-29a-5p	Down	*HDAC9*	N/A
hsa-miR-211-5p	Not significant	*HDAC9*	N/A
hsa-miR-3619-5p	Up	*HDAC9*	No change
hsa-miR-30c-5p	Down	*JAK1*	N/A
hsa-miR-9-5p	Up	*JAK1*	N/A
hsa-miR-373-3p	Not significant	*JAK1*	N/A
hsa-miR-107*	Up	*JAK1*	N/A
hsa-miR-126-3p	Down	*JAK1*	N/A
hsa-miR-106b-5p	Up	*JAK1*	No change
hsa-miR-17-5p	Up	*JAK1*	No change
hsa-miR-452-5p	Up	*LEF1*	N/A
hsa-miR-218-5p	Not significant	*LEF1*	N/A
hsa-miR-34c-3p	Up	*LEF1*	Up
hsa-miR-34a-5p	Up	*LEF1*	Up
hsa-miR-449a*	Up	*LEF1*	Up
hsa-let-7i-3p	Not significant	*LEF1*	N/A
hsa-miR-186-5p	Not significant	*MOB1A*	N/A
hsa-miR-199a-5p	Down	*SMARCA2*	N/A
hsa-miR-199a-3p	Down	*SMARCA2*	N/A
hsa-miR-18a-5p	Up	*STK4*	N/A
hsa-miR-655-3p	Down	*VIM-AS1*	N/A

significant are indicated by N/A and Not significance, respectively. Additional information about this analysis is provided in Appendix 7.

The sequences of these 24 miRNAs were validated against different transcripts of LncRNA, circRNA, as well as their corresponding mRNA transcripts from the previous stage using lncTar analysis. The details can be found in the attached document.

The Human MicroRNA Disease Database (HMDD v4.0) offers a comprehensive and expanded collection of miRNA-disease associations with improved classification and new features for network visualization. By searching the HMDD v4.0 database [86], it was found that two miRNAs, *hsa-mir-107* and *hsa-miR-449a*, are associated with hepatocellular carcinoma causality and these are indicated with an asterisk (*) in Table 5. The networks of these two miRNAs can be observed in Fig. 7.

Our analysis revealed a complex network of interactions between the selected genes, microRNAs, lncRNAs, and circRNA. Notably, 24 microRNAs showed interactions with 9 of our selected genes (7 initially identified plus *PRKCB* and *DLG1*). Furthermore, all 10

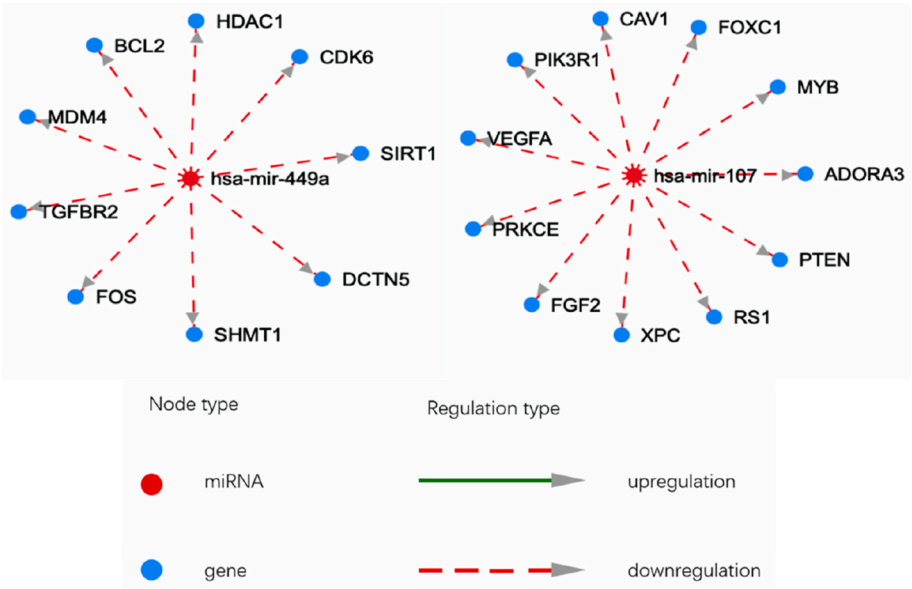

Fig. 7. miRNA regulatory network involving *hsa-miR-107* and *hsa-miR-449a*.

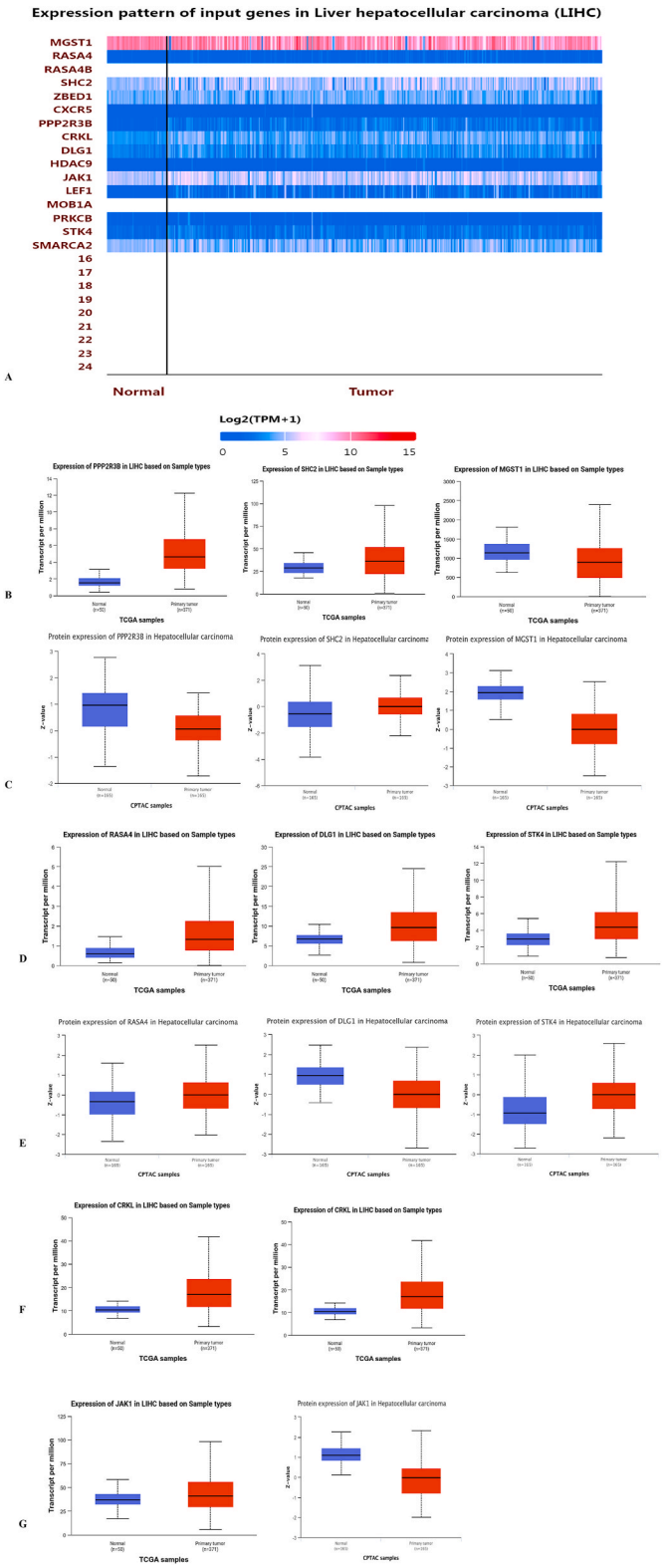

Fig. 8. Heatmap of gene expression using TCGA-LIHC dataset, highlighting statistically significant results for both gene and protein expression. (A) Heatmap displaying gene expression patterns of up-regulated and down-regulated genes in liver hepatocellular carcinoma. (B) Gene expression levels for *PPP2RB3, SHC2, MGST1* (C) Protein expression levels for PPP2RB3, SHC2, MGST1 (D) Gene expression levels for *RASA4, DLG1, STK4* (E) Protein expression levels for RASA4, DLG1, STK4 (F) Gene and protein expression for gene *CRKL* (G) Gene and protein expression for gene *JAK1*.

lncRNAs showed physical interactions with these microRNAs. Interestingly, the selected *hsa_circ_0001380* interacted with all the microRNAs except one (*hsa-miR-30c-5p*). Fig. 4 provides a visualization of these interactions.

The genes listed in Tables 3 and 4, derived from co-expression networks and differentially expressed gene (DEG) analysis in exosomes, were searched on the UALCAN website [26].

Fig. 8 presents a comprehensive visualization and analysis of gene expression patterns in hepatocellular carcinoma using the TCGA-LIHC dataset. The heatmap (A) displays the expression patterns of 16 key genes that were identified through our RNA-RNA interaction analysis and subsequently queried in UALCAN portal. This analysis provided both transcriptomic and proteomic data from TCGA for these specific genes, allowing us to examine their expression patterns in HCC compared to normal tissue. Subsequent panels (B-G) provide detailed expression analyses for selected genes, showing both their transcriptional and protein-level regulation in HCC, which helps elucidate their potential roles in disease progression. These selected genes showed particularly interesting patterns of dysregulation and were further analyzed to understand their contribution to HCC pathogenesis.

A summary of gene and protein expression patterns is provided in Table 6.

The heatmap in this figure was generated using data from UALCAN. Please refer to the UALCAN manuscript for further details. More information is available at https://ualcan.path.uab.edu.

Table 6 provides computational expression profiles from tissue studies of hepatocellular carcinoma. Data were extracted from UALCAN.

3.8. Statistical analysis enhancement

The statistical analysis was conducted using R version 4.2.2 and the Relative Expression Software Tool (REST-2009). Gene expression analyses, including normalization, filtering, and differentially expressed gene (DEG) analysis, were performed using R software. In the investigation of physical interactions between RNAs, the guidelines provided by LncTAR were adhered to, setting the threshold for the normal ΔG cutoff at −0.15. For protein-protein interaction (PPI) analysis, the STRING database was utilized, and for miRNA interaction analysis, the miRTarBase online database was used. Differential expression of genes between sample groups was assessed using the linear model method, with statistical significance determined by false discovery rate (FDR) adjustment (FDR <0.01). The significance of other statistical analyses was assessed with a p-value threshold of <0.05.

4. Discussion

Hepatocellular carcinoma (HCC) remains a formidable challenge in global health, characterized by complex molecular mechanisms driving its progression [87]. This study presents a comprehensive analysis of gene expression patterns and regulatory networks in HCC, integrating data from tissue samples and exosomes while exploring the intricate web of interactions among various RNA species, including mRNAs, lncRNAs, circRNAs, and miRNAs. Our analysis revealed a complex network of predicted physical interactions among these RNA species. Notably, we found that exosomal RNA content can reliably reflect tissue-specific gene expression changes, highlighting the potential of exosomes for non-invasive diagnostics. Key genes such *as MOB1A, HDAC9, PRKCB, STK4, SMARCA2*, and *JAK1* showed interactions with multiple miRNAs, suggesting intricate regulatory mechanisms in HCC pathogenesis.

These findings both confirm and expand upon previous research in the field of HCC and exosomal RNA. Our observations on the role of *RN7SL1* in activating the RIG-I pathway and stimulating an interferon response, which paradoxically promotes tumor progression, align with the study by Nabet et al. (2017) [88]. Furthermore, our findings on the importance of *JAK1*, and *CRKL* in multiple signaling pathways corroborate and extend previous findings on the role of these genes in HCC progression [55,89].

4.1. Expression patterns and RNA-RNA interactions

These analysis revealed diverse expression patterns across different genes, underscoring the complexity of gene regulation in HCC [90]. The consistency observed in gene expression patterns between tissue samples and exosomes suggests that exosomal RNA content reliably reflects tissue-specific gene expression changes, making exosomes a promising tool for non-invasive diagnostics [91].

However, discrepancies between mRNA and protein levels were observed in some cases, highlighting the complexity of post-transcriptional regulation in HCC. For instance.

- ***PRKCB*** showed reductions in both mRNA and protein levels, potentially due to its interaction with ***RN7SL1* transcripts** and ***lnc-C12orf74-3:34*.**
- ***SMARCA2***, on the other hand, exhibited reduced mRNA levels but increased protein expression, possibly influenced by its interaction with ***hsa_circ_0001380*.**

These observations extend our understanding of the intricate regulatory mechanisms in HCC, suggesting that post-transcriptional factors, selective exosomal packaging, and tumor microenvironment dynamics play significant roles.

4.2. Implications for signaling pathways and tumor microenvironment

The expression patterns and interactions observed in this study have significant implications for various signaling pathways and the tumor microenvironment (TME).

Table 6
Summary of gene expression data.

Gene	HCC RNA Tissue Expression	Normal Protein Level	HCC Protein Level	References
PRKCB	Down	High	Low	UALCAN.
HDAC9	NA	NA	NA	UALCAN.
SMARCA2	NA	Low	High	UALCAN.
LEF1	Up	NA	NA	UALCAN.
DLG1	Up	High	Low	UALCAN.
CRKL	Up	Low	High	UALCAN.
JAK1	Up	High	Low	UALCAN.
MOB1A	Up	Low	High	UALCAN.
STK4	Up	Low	High	UALCAN.
MGST1	Down	High	Low	UALCAN.
CXCR5	NA	NA	NA	UALCAN.
ZBED1	NA	NA	NA	UALCAN.
RASA4	Up	Low	High	UALCAN.
SHC2	Up	Low	High	UALCAN.
PPP2R3B	Up	High	Low	UALCAN.

1. Perturbations in multiple signaling pathways, including PKC and JAK/STAT cascades, are indicated by changes in expression and interactions of ***PRKCB***, ***JAK1***, and ***CRKL*** [55,67,75]. These pathways play pivotal roles in regulating immune evasion, angiogenesis, and apoptosis within the TME.
2. The selective inclusion of RNA species in exosomes suggests a mechanism by which HCC cells actively shape the TME. For instance, ***RN7SL1*** was found to activate the RIG-I pathway, stimulating an interferon response that paradoxically promotes tumor progression [88].
3. Dysregulation of ***DLG1*** and its interactions with multiple lncRNAs suggest a complex regulatory network controlling cell polarity and intercellular interactions, potentially impacting metastasis [92].
4. The interactions of key non-coding RNAs, such as ***lnc-C12orf74-3:34*** and ***hsa_circ_0001380***, with genes like ***PRKCB*** and ***SMARCA2***, further emphasize their roles in modulating signaling pathways and the microenvironment. These findings underscore the dynamic interplay between tumor cells and the TME, mediated through exosomal communication.

These results not only highlight the relevance of ncRNAs in the TME but also provide a foundation for further experimental studies to validate these mechanisms and explore their potential as therapeutic targets.

4.3. Potential therapeutic applications of exosomal communication

A deeper understanding of the messages cancer cells send to distant sites through exosomes can provide novel therapeutic approaches [93]. Exosomes, as carriers of molecular signals, might play a crucial role in preparing distant sites for metastasis or modulating immune responses [94]. By deciphering the specific messages and molecular contents within these exosomes, we could potentially develop targeted therapies that interrupt these communication pathways. This approach may offer new treatment options that go beyond conventional systemic chemotherapy, particularly for cancers where current treatments are limited [95].

These findings provide new insights into the molecular basis of HCC progression and may offer novel targets for therapeutic intervention.

4.4. Role of non-coding RNAs and exosomes

Our study uncovered a complex network of predicted physical interactions among various RNA species. Key genes such as *MOB1A, HDAC9, PRKCB, STK4, SMARCA2*, and *JAK1* showed interactions with multiple miRNAs, including *hsa-miR-29a-3p, hsa-miR-124-3p,* and *hsa-miR-15a-5p.* These interactions can play a significant role in regulating gene expression and cellular pathways [96].

Further analysis using the miRTarBase database revealed an even more intricate network of interactions. We identified 24 microRNAs that showed interactions with 9 of our selected genes (*MGST1, RASA4, RASA4B, SHC2, ZBED1, CXCR5, PPP2R3B, CRKL, DLG1, HDAC9, JAK1, LEF1, MOB1A, PRKCB, STK4, SMARCA2*). Interestingly, these microRNAs also showed physical interactions with 10 lncRNAs and one circRNA that we identified in our study. Notably, all lncRNAs interacted with all 24 microRNAs, while the circRNA interacted with all except *hsa-miR-30c-5p*. This complex interactome suggests a highly coordinated regulatory network involving various RNA species in HCC, potentially influencing gene expression and cellular pathways through competitive binding or co-regulation mechanisms.

The differential expression patterns observed between exosomes and cellular samples highlight the selective nature of exosomal packaging [97]. This suggests a mechanism by which cancer cells might modulate the tumor microenvironment, potentially priming distant sites for metastasis or influencing immune cell functions [93]. These findings open new avenues for understanding intercellular communication in HCC and may lead to novel diagnostic and therapeutic strategies.

In our analysis of non-coding RNAs, we designed primers to detect specific transcripts of interest. Notably, our primer sets for *VIM-AS1* were able to detect transcripts *VIM-AS1:14, VIM-AS1:16*, and *VIM-AS1:17*, which showed 100 % sequence similarity in BLAST

analysis. Similarly, primers for *SEMA3F-AS1* detected both *SEMA3F-AS1:2* and *SEMA3F-AS1:3* transcripts, which also exhibited 100 % similarity. For *RN7SL1*, our primers were designed to capture both *lnc-LRR1-1:1* and *lnc-LRR1-1:2* transcripts, which showed 99 % similarity. This high degree of similarity between transcripts of the same gene highlights the complexity of transcriptional regulation in HCC and underscores the importance of careful primer design in studying non-coding RNAs. The detection of these highly similar transcripts raises intriguing questions about their functional roles and potential differences in regulation or interaction with other RNA species in the context of HCC progression.

Our network analysis revealed a complex web of interactions among various RNA species in HCC (Fig. 4). To simplify the visual representation, we depicted the 24 identified miRNAs as a single node. Notably, all examined genes and lncRNAs showed interactions with the entire set of 24 miRNAs, suggesting a highly interconnected regulatory network.

Interestingly, the identified *hsa_circ_0001380* exhibited interactions with 23 out of the 24 miRNAs, with the sole exception being *hsa-miR-30c-5p*. This comprehensive interaction pattern underscores the potential for intricate regulatory mechanisms in HCC, where multiple RNA species may compete for miRNA binding or cooperate in gene expression regulation.

Among these miRNAs, Table 5 highlights specific interactions, including those of *hsa-miR-107** (targeting *CRKL* and *JAK1*) and *hsa-miR-449a** (targeting *LEF1*). These miRNAs and their targets exhibit particular expression patterns in LIHC in TCGA, indicating potential regulatory roles in liver cancer pathogenesis.

The unique interaction profile of *hsa_circ_0001380*, particularly its lack of interaction with *hsa-miR-30c-5p*, warrants further investigation as it may indicate a specific regulatory role or functional significance in HCC pathogenesis. These findings provide a foundation for further research into the complex miRNA-mRNA-lncRNA-circRNA regulatory networks in HCC and their potential as diagnostic or therapeutic targets.

4.5. Limitations and future directions

The RNA-seq data used lacks detailed patient disease stages and clinical conditions. Moreover, the exosomes sequenced from blood samples may originate from non-liver sources, emphasizing the need for liver-specific exosome studies. Our BLAST analysis revealed 100 % sequence similarity among certain transcripts (e.g., *VIM-AS1:14, VIM-AS1:16*, and *VIM-AS1:17; SEMA3F-AS1:2* and *SEMA3F-AS1:3*), allowing us to design primers that effectively detect these highly similar isoforms. While our method successfully identified these similar transcripts, it raises questions about the biological significance of such closely related isoforms. Future studies could employ more advanced techniques, such as isoform-specific sequencing or functional assays, to examine the potential distinct roles or regulatory mechanisms of these highly similar transcripts. The biological implications of these subtle transcript variations in HCC progression remain to be fully elucidated and warrant further investigation. Future research should focus on.

1. Validating these findings in larger cohorts of liver cancer patients, correlating ncRNA expression levels with clinical outcomes.
2. Conducting functional analyses of identified ncRNAs to elucidate their specific roles in liver cancer progression.
3. Developing reliable and non-invasive biomarkers based on the identified ncRNAs for early detection and monitoring of liver cancer.
4. Investigating the potential of targeting these ncRNAs for therapeutic purposes, including the development of ncRNA-based therapies.
5. Integrating these findings with emerging technologies such as AI to enhance HCC research and treatment strategies.

While the focus of this study was on hepatocellular carcinoma (HCC), several of the identified genes and non-coding RNAs (ncRNAs) have been implicated in other cancer types as well. For instance, *CRKL* and *PRKCB* are known to influence key pathways such as JAK/STAT and PKC, which are dysregulated in cancers like colorectal, lung, and breast cancers. Similarly, pathways like PI3K-Akt and Ras signaling, which were highlighted in our analysis, are commonly affected across various malignancies.

However, a systematic comparison of these findings with other cancer types was beyond the scope of this study. Future research could focus on exploring the broader relevance of these ncRNAs and pathways across different cancers, potentially uncovering shared mechanisms and therapeutic targets.

4.6. Clinical implications

The identification of novel candidate biomarkers, including *lnc-HMGA1-2:8, lnc-HMGA1-2:9*, and *lnc-C12orf74-3:34*, reported here for the first time, alongside the confirmed differential expression of *hsa_circ_0001380, SEMA3F-AS1:2,3, lnc-LRR1-1:1,2,* and *VIM-AS1:14*, underscores the potential of non-coding RNAs in enhancing our understanding of liver cancer pathogenesis. These findings may lead to the development of new diagnostic tools and therapeutic targets, potentially improving patient outcomes in HCC.

5. Conclusion

This comprehensive analysis reveals an extraordinarily complex and interconnected RNA regulatory network in HCC, highlighting the importance of non-coding RNAs and exosomal communication in disease progression. Our findings not only deepen the understanding of HCC pathogenesis but also open up new avenues for biomarker discovery and therapeutic interventions. By pursuing integrated future directions, we can advance towards more personalized and effective treatments for HCC patients.

CRediT authorship contribution statement

Farzin Mirzaei-nasab: Writing – original draft, Resources, Methodology, Investigation, Data curation, Conceptualization. **Ahmad Majd:** Writing – original draft, Validation, Data curation. **Yousef Seyedena:** Writing – original draft, Validation, Software, Methodology. **Nazanin Hosseinkhan:** Writing – review & editing, Visualization, Validation, Supervision. **Najma Farahani:** Writing – review & editing, Supervision. **Mehrdad Hashemi:** Writing – review & editing, Validation, Supervision, Conceptualization.

Data availability

"The datasets analyzed during the current study are available in the Gene Expression Omnibus (GEO) repository, [GSE100206 and GSE100207]".

https://www.ncbi.nlm.nih.gov/geo/query/acc.cgi?acc=GSE100206

https://www.ncbi.nlm.nih.gov/geo/query/acc.cgi?acc=GSE100207.

(also The datasets (Normal and HCC) analyzed during the current study are available in the http://www.exorbase.org/repository, http://www.exorbase.org:9000/exoRBase/download/toIndex)

Ethics

To respect the rights of patients, the present study was approved by the ethics committee of the Islamic Azad University, North Tehran branch, with the code of ethics IR.IAU.TNB. REC.1400/056.

Declaration of competing interest

The authors declare that they have no known competing financial interests or personal relationships that could have appeared to influence the work reported in this paper.

Appendix A. Supplementary data

Supplementary data to this article can be found online at https://doi.org/10.1016/j.plabm.2025.e00464.

Data availability

Data will be made available on request.

References

[1] W.H. Organization, Definition, Diagnosis and Classification of Diabetes Mellitus and its Complications: Report of a WHO Consultation. Part 1, Diagnosis and Classification of Diabetes Mellitus, World health organization, 1999.
[2] B. Zhang, R.W.Y. Yeo, R.C. Lai, E.W.K. Sim, K.C. Chin, S.K. Lim, Mesenchymal stromal cell exosome–enhanced regulatory T-cell production through an antigen-presenting cell–mediated pathway, Cytotherapy 20 (5) (2018) 687–696.
[3] X. Yu, et al., Exosomal non-coding RNAs in colorectal cancer metastasis, Clin. Chim. Acta (2024) 117849.
[4] W. Lim, H.-S. Kim, Exosomes as therapeutic Vehicles for cancer, Tissue Eng. Regen. Med. 16 (2019) 213–223.
[5] M. Işın, et al., Exosomal lncRNA-p21 levels may help to distinguish prostate cancer from benign disease, Front. Genet. 6 (2015) 168.
[6] M. Dragomir, B. Chen, G.A. Calin, Exosomal lncRNAs as new players in cell-to-cell communication, Transl. Cancer Res. 7 (Suppl 2) (2018) S243.
[7] B. Zhu, et al., Stem cell-derived exosomes prevent aging-induced cardiac dysfunction through a novel exosome/lncRNA MALAT1/NF-κB/TNF-α signaling pathway, Oxid. Med. Cell. Longev. 2019 (1) (2019) 9739258.
[8] T. Fan, N. Sun, J. He, Exosome-derived lncRNAs in lung cancer, Front. Oncol. 10 (2020) 1728.
[9] Y. Wang, et al., Exosomal circRNAs: biogenesis, effect and application in human diseases, Mol. Cancer 18 (2019) 1–10.
[10] W. Chen, et al., Exosome-transmitted circular RNA hsa_circ_0051443 suppresses hepatocellular carcinoma progression, Cancer Lett. 475 (2020) 119–128.
[11] X. Yu, S.L. Harris, A.J. Levine, The regulation of exosome secretion: a novel function of the p53 protein, Cancer Res. 66 (9) (2006) 4795–4801.
[12] L. Milane, A. Singh, G. Mattheolabakis, M. Suresh, M.M. Amiji, Exosome mediated communication within the tumor microenvironment, J. Control. Release 219 (2015) 278–294.
[13] M. Zhou, X. He, C. Mei, C. Ou, Exosome derived from tumor-associated macrophages: biogenesis, functions, and therapeutic implications in human cancers, Biomark. Res. 11 (1) (2023) 100.
[14] T.L. Whiteside, Exosomes and tumor-mediated immune suppression, J. Clin. Investig. 126 (4) (Feb. 2016) 1216–1223.
[15] M.N. Huda, et al., Potential use of exosomes as diagnostic biomarkers and in targeted drug delivery: progress in clinical and preclinical applications, ACS Biomater. Sci. Eng. 7 (6) (2021) 2106–2149.
[16] I. Zwiener, B. Frisch, H. Binder, Transforming RNA-Seq data to improve the performance of prognostic gene signatures, PLoS One 9 (1) (Jan. 2014) e85150.
[17] I. Zwiener, B. Frisch, H. Binder, Transforming RNA-Seq data to improve the performance of prognostic gene signatures, PLoS One 9 (1) (Jan. 2014).
[18] A. Ramasamy, A. Mondry, C.C. Holmes, D.G. Altman, Key issues in conducting a meta-analysis of gene expression microarray datasets, PLoS Med. 5 (9) (2008) e184.
[19] B. Zhang, S. Horvath, A General Framework for Weighted Gene Co-expression Network Analysis, 2005.
[20] E. Ravasz, A.L. Somera, D.A. Mongru, Z.N. Oltvai, A.-L. Barabási, Hierarchical organization of modularity in metabolic networks, Science 297 (5586) (2002) 1551–1555.

[21] P. Langfelder, B. Zhang, S. Horvath, Defining clusters from a hierarchical cluster tree: the Dynamic Tree Cut package for R, Bioinformatics 24 (5) (2008) 719–720.
[22] M.E. Ritchie, et al., Limma powers differential expression analyses for RNA-sequencing and microarray studies, Nucleic Acids Res. 43 (7) (2015) e47–e47.
[23] J. Li, et al., LncTar: a tool for predicting the RNA targets of long noncoding RNAs, Brief. Bioinform. 16 (5) (2014) 806–812.
[24] M. Kanehisa, S. Goto, KEGG: kyoto encyclopedia of genes and genomes, Nucleic Acids Res. 28 (1) (2000) 27–30.
[25] Z. Xie, et al., Gene set knowledge discovery with Enrichr, Curr. Protoc. 1 (3) (2021) e90.
[26] D.S. Chandrashekar, et al., UALCAN: a portal for facilitating tumor subgroup gene expression and survival analyses, Neoplasia 19 (8) (2017) 649–658.
[27] M. Kanehisa, Toward understanding the origin and evolution of cellular organisms, Protein Sci. 28 (11) (2019) 1947–1951.
[28] M. Kanehisa, M. Furumichi, Y. Sato, M. Kawashima, M. Ishiguro-Watanabe, KEGG for taxonomy-based analysis of pathways and genomes, Nucleic Acids Res. 51 (D1) (2023) D587–D592.
[29] D.J.B. Clarke, et al., Appyters: turning jupyter notebooks into data-driven web apps, Patterns 2 (3) (2021).
[30] E.Y. Chen, et al., Enrichr: interactive and collaborative HTML5 gene list enrichment analysis tool, BMC Bioinf. 14 (2013) 1–14.
[31] M.V. Kuleshov, et al., Enrichr: a comprehensive gene set enrichment analysis web server 2016 update, Nucleic Acids Res. 44 (W1) (2016) W90–W97.
[32] Paula Takahashi, et al., MicroRNA expression profiling and functional annotation analysis of their targets in patients with type 1 diabetes mellitus, Gene 539 (2) (2014) 213–223.
[33] P. Shannon, et al., Cytoscape: a software environment for integrated models of biomolecular interaction networks, Genome Res. 13 (11) (2003) 2498–2504.
[34] P. Cai, et al., MGST1 overexpression promotes hepatocellular carcinoma development, Basic & Clin. Med. 38 (7) (2018) 950.
[35] S. Maran, et al., Gastric precancerous lesions are associated with gene variants in Helicobacter pylori-susceptible ethnic Malays, World J. Gastroenterol. WJG 19 (23) (2013) 3615.
[36] F. Kuang, J. Liu, Y. Xie, D. Tang, R. Kang, MGST1 is a redox-sensitive repressor of ferroptosis in pancreatic cancer cells, Cell Chem. Biol. 28 (6) (2021) 765–775.
[37] H. Zhang, et al., Microsomal glutathione S-transferase gene polymorphisms and colorectal cancer risk in a Han Chinese population, Int. J. Colorectal Dis. 22 (10) (2007) 1185–1194.
[38] D.F. Calvisi, et al., Inactivation of Ras GTPase-activating proteins promotes unrestrained activity of wild-type Ras in human liver cancer, J. Hepatol. 54 (2) (2011) 311–319.
[39] J. Chen, J. Huang, Q. Huang, J. Li, E. Chen, W. Xu, RASA4 inhibits the HIFα signaling pathway to suppress proliferation of cervical cancer cells, Bioengineered 12 (2) (2021) 10723–10733.
[40] Y. Wang, Y.-X. Qi, Z. Qi, S.-Y. Tsang, TRPC3 regulates the proliferation and apoptosis resistance of triple negative breast cancer cells through the TRPC3/RASA4/MAPK pathway, Cancers 11 (4) (2019) 558.
[41] S. Whittaker, R. Marais, A.X. Zhu, The role of signaling pathways in the development and treatment of hepatocellular carcinoma, Oncogene 29 (36) (2010) 4989–5005.
[42] J. Ramos, et al., NRF1 motif sequence-enriched genes involved in ER/PR− ve HER2+ ve breast cancer signaling pathways, Breast Cancer Res. Treat. 172 (2) (2018) 469–485.
[43] P. Yang, W. Li, X. Li, SHC1 promotes lung cancer metastasis by interacting with EGFR, J. Oncol. 2022 (2022).
[44] S. Jiang, Y. Wang, Y. Xiong, Y. Feng, J. Tang, R. Song, High expression of ZBED1 affects proliferation and apoptosis in gastric cancer, Int. J. Clin. Exp. Pathol. 11 (8) (2018) 4019.
[45] S. Johansen, et al., ZBED1 regulates genes important for multiple biological processes of the placenta, Genes 13 (1) (2022) 133.
[46] K. Hagiwara, et al., A new liver-regeneration molecular mechanism involving hepatic stellate cells, kupffer cells, and glucose-regulated protein 78 as a new hepatotrophic factor, J. Hepato-Biliary-Pancreatic Sci. 30 (2) (2023) 16–176.
[47] Z.-Q. Zhou, et al., Follicular helper T cell exhaustion induced by PD-L1 expression in hepatocellular carcinoma results in impaired cytokine expression and B cell help, and is associated with advanced tumor stages, Am. J. Transl. Res. 8 (7) (2016) 2926.
[48] R. Singh, P. Gupta, G.H. Kloecker, S. Singh, J.W. Lillard Jr., Expression and clinical significance of CXCR5/CXCL13 in human non-small cell lung carcinoma, Int. J. Oncol. 45 (6) (2014) 2232–2240.
[49] S. Singh, et al., Clinical and biological significance of CXCR5 expressed by prostate cancer specimens and cell lines, Int. J. Cancer 125 (10) (2009) 2288–2295.
[50] Q. Yan, et al., The expression and significance of CXCR5 and MMP-13 in colorectal cancer, Cell Biochem. Biophys. 73 (1) (2015) 253–259.
[51] Y. Ding, J. Shen, G. Zhang, X. Chen, J. Wu, W. Chen, CD40 controls CXCR5-induced recruitment of myeloid-derived suppressor cells to gastric cancer, Oncotarget 6 (36) (2015) 38901.
[52] W. Chen, Z. Wang, C. Jiang, Y. Ding, PP2A-mediated anticancer therapy, Gastroenterol. Res. Pract. 2013 (2013).
[53] L.C.L. van Kempen, et al., The protein phosphatase 2A regulatory subunit PR70 is a gonosomal melanoma tumor suppressor gene, Sci. Transl. Med. 8 (369) (2016), 369ra177-369ra177.
[54] H. Li, L.-L. Zhao, J.W. Funder, J.-P. Liu, Protein phosphatase 2A inhibits nuclear telomerase activity in human breast cancer cells, J. Biol. Chem. 272 (27) (1997) 16729–16732.
[55] Z. Peng, X. Ouyang, Y. Wang, Q. Fan, MAPKAPK5-AS1 drives the progression of hepatocellular carcinoma via regulating miR-429/ZEB1 axis, BMC Mol. Cell Biol. 23 (1) (2022) 1–11.
[56] Y.H. Kim, et al., Genomic and functional analysis identifies CRKL as an oncogene amplified in lung cancer, Oncogene 29 (10) (2010) 1421–1430.
[57] T. Zhao, et al., Overexpression of CRKL correlates with malignant cell proliferation in breast cancer, Tumor Biol. 34 (5) (2013) 2891–2897.
[58] J. Wang, et al., CRKL promotes cell proliferation in gastric cancer and is negatively regulated by miR-126, Chem. Biol. Interact. 206 (2) (2013) 230–238.
[59] Q. Song, et al., CRKL regulates alternative splicing of cancer-related genes in cervical cancer samples and HeLa cell, BMC Cancer 19 (1) (2019) 1–16.
[60] X. Xiaoli, Z. Haoxiong, Y. Bilan, W. Bin, Y. Yidong, LRRC1 promotes proliferation of hepatocellular carcinoma cells via DLG1/YAP signaling pathway, J. NEW Med. 52 (4) (2021) 272.
[61] M.D. Beckler, et al., Proteomic analysis of exosomes from mutant KRAS colon cancer cells identifies intercellular transfer of mutant KRAS, Mol. Cell. proteomics 12 (2) (2013) 343–355.
[62] B. Liang, et al., Characterization and proteomic analysis of ovarian cancer-derived exosomes, J. Proteomics 80 (2013) 171–182.
[63] P. Kharaziha, et al., Molecular profiling of prostate cancer derived exosomes may reveal a predictive signature for response to docetaxel, Oncotarget 6 (25) (2015) 21740.
[64] Y. Zheng, et al., MiR-376a and histone deacetylation 9 form a regulatory circuitry in hepatocellular carcinoma, Cell. Physiol. Biochem. 35 (2) (2015) 729–739.
[65] M. Lapierre, et al., Histone deacetylase 9 regulates breast cancer cell proliferation and the response to histone deacetylase inhibitors, Oncotarget 7 (15) (2016) 19693.
[66] Z. Ma, et al., Histone deacetylase 9 downregulation decreases tumor growth and promotes apoptosis in non-small cell lung cancer after melatonin treatment, J. Pineal Res. 67 (2) (2019) e12587.
[67] B.W.M. van Balkom, A.S. Eisele, D.M. Pegtel, S. Bervoets, M.C. Verhaar, Quantitative and qualitative analysis of small RNAs in human endothelial cells and exosomes provides insights into localized RNA processing, degradation and sorting, J. Extracell. Vesicles 4 (1) (2015) 26760.
[68] H. Peinado, et al., Melanoma exosomes educate bone marrow progenitor cells toward a pro-metastatic phenotype through MET, Nat. Med. 18 (6) (2012) 883–891.
[69] L. Sun, T. Liu, S. Zhang, K. Guo, Y. Liu, Oct4 induces EMT through LEF1/β-catenin dependent WNT signaling pathway in hepatocellular carcinoma, Oncol. Lett. 13 (4) (2017) 2599–2606.
[70] J. Liang, et al., LEF1 targeting EMT in prostate cancer invasion is regulated by miR-34aLEF1 in prostate cancer EMT by miR-34a, Mol. Cancer Res. 13 (4) (2015) 681–688.
[71] W.-J. Wang, et al., Increased LEF1 expression and decreased Notch2 expression are strong predictors of poor outcomes in colorectal cancer patients, Dis. Markers 35 (5) (2013) 395–405.

[72] Y. Liu, X. Wang, Y. Yang, Hepatic Hippo signaling inhibits development of hepatocellular carcinoma, Clin. Mol. Hepatol. 26 (4) (2020) 742.
[73] P. Yang, et al., CAF-derived exosomal WEE2-AS1 facilitates colorectal cancer progression via promoting degradation of MOB1A to inhibit the Hippo pathway, Cell Death Dis. 13 (9) (2022) 1–14.
[74] B. Yang, et al., MOB1A regulates glucose deprivation-induced autophagy via IL6-STAT3 pathway in gallbladder carcinoma, Am. J. Cancer Res. 10 (11) (2020) 3896.
[75] M. He, et al., Hepatocellular carcinoma-derived exosomes promote motility of immortalized hepatocyte through transfer of oncogenic proteins and RNAs, Carcinogenesis 36 (9) (2015) 1008–1018.
[76] W. Li, et al., STK4 regulates TLR pathways and protects against chronic inflammation–related hepatocellular carcinoma, J. Clin. Investig. 125 (11) (2015) 4239–4254.
[77] L. Yang, J. Wu, M. Guo, Y. Zhang, S. Ma, Suppression of long non-coding RNA TNRC6C-AS1 protects against thyroid carcinoma through DNA demethylation of STK4 via the Hippo signalling pathway, Cell Prolif. 52 (3) (2019) e12564.
[78] T.I. Hsu, et al., MicroRNA-18a is elevated in prostate cancer and promotes tumorigenesis through suppressing STK4 in vitro and in vivo, Oncogenesis 3 (4) (2014) e99–e99.
[79] W. Zhao, H. Mo, R. Liu, T. Chen, N. Yang, Z. Liu, Matrix stiffness-induced upregulation of histone acetyltransferase KAT6A promotes hepatocellular carcinoma progression through regulating SOX2 expression, Br. J. Cancer (2022) 1–9.
[80] W. Liu, et al., KAT6A, a novel regulator of β-catenin, promotes tumorigenicity and chemoresistance in ovarian cancer by acetylating COP1, Theranostics 11 (13) (2021) 6278.
[81] Q. He, J. Yang, Y. Jin, Immune infiltration and clinical significance analyses of the coagulation-related genes in hepatocellular carcinoma, Brief. Bioinform. 23 (4) (2022).
[82] S. Keerthikumar, et al., Proteogenomic analysis reveals exosomes are more oncogenic than ectosomes, Oncotarget 6 (17) (2015) 15375.
[83] E. Herpel, et al., SMARCA4 and SMARCA2 deficiency in non–small cell lung cancer: immunohistochemical survey of 316 consecutive specimens, Ann. Diagn. Pathol. 26 (2017) 47–51.
[84] Z. Zhang, et al., BRM/SMARCA2 promotes the proliferation and chemoresistance of pancreatic cancer cells by targeting JAK2/STAT3 signaling, Cancer Lett. 402 (2017) 213–224.
[85] S.-D. Hsu, et al., miRTarBase: a database curates experimentally validated microRNA–target interactions, Nucleic Acids Res. 39 (suppl_1) (2011) D163–D169.
[86] Z. Huang, et al., HMDD v3. 0: a database for experimentally supported human microRNA–disease associations, Nucleic Acids Res. 47 (D1) (2019) D1013–D1017.
[87] J. Balogh, et al., Hepatocellular carcinoma: a review, J. Hepatocell. Carcinoma 3 (Oct. 2016) 41.
[88] B.Y. Nabet, et al., Exosome RNA unshielding couples stromal activation to pattern recognition receptor signaling in cancer, Cell 170 (2) (2017) 352–366.
[89] Y. Xu, et al., Exosomal miR-200b-3p induce macrophage polarization by regulating transcriptional repressor ZEB1 in hepatocellular carcinoma, Hepatol. Int. 17 (4) (2023) 889–903.
[90] T.A. Dragani, Risk of HCC: genetic heterogeneity and complex genetics, J. Hepatol. 52 (2) (2010) 252–257.
[91] A. Roychowdhury, Exosomal RNA as a biomarker in cancer diagnostics and therapy, in: Exosomal RNA, Elsevier, 2024, pp. 85–109.
[92] C. Andolfi, C. Tiribelli, D. Pascut, Recent hints on the dual role of discs large MAGUK scaffold protein 5 in cancers and in hepatocellular carcinoma, Front. Biosci. 27 (5) (2022) 164.
[93] Z. Wan, et al., Exosome-mediated cell-cell communication in tumor progression, Am. J. Cancer Res. 8 (9) (2018) 1661–1673.
[94] M.C. Knox, et al., A clinician's guide to cancer-derived exosomes: immune interactions and therapeutic implications, Front. Immunol. 11 (Jul. 2020) 1612.
[95] M.D.A. Paskeh, et al., Emerging role of exosomes in cancer progression and tumor microenvironment remodeling, BioMed Central 15 (1) (2022).
[96] J. Long, C. Jiang, B. Liu, S. Fang, M. Kuang, MicroRNA-15a-5p suppresses cancer proliferation and division in human hepatocellular carcinoma by targeting BDNF, Tumor Biol. 37 (2016) 5821–5828.
[97] J. Daßler-Plenker, V. Küttner, M. Egeblad, Communication in tiny packages: exosomes as means of tumor-stroma communication, Biochim. Biophys. Acta (BBA)-Reviews Cancer 1873 (2) (2020) 188340.